Title
KRIT-1/CCM1 is a Rap1 effector that regulates endothelial cell–cell junctions

Journal
Journal of Cell Biology, 179(2)

ISSN
0021-9525

Authors
Glading, Angela
Han, Jaewon
Stockton, Rebecca A
et al.

Publication Date
2007-10-22

DOI
10.1083/jcb.200705175

Peer reviewed

KRIT-1/CCM1 is a Rap1 effector that regulates endothelial cell–cell junctions

Angela Glading, Jaewon Han, Rebecca A. Stockton, and Mark H. Ginsberg

Department of Medicine, University of California, San Diego, La Jolla, CA 92093

Cerebral cavernous malformation (CCM), a disease associated with defective endothelial junctions, result from autosomal dominant CCM1 mutations that cause loss of KRIT-1 protein function, though how the loss of KRIT-1 leads to CCM is obscure. KRIT-1 binds to Rap1, a guanosine triphosphatase that maintains the integrity of endothelial junctions. Here, we report that KRIT-1 protein is expressed in cultured arterial and venous endothelial cells and is present in cell–cell junctions. KRIT-1 colocalized and was physically associated with junctional proteins via its band 4.1/ezrin/radixin/moesin (FERM) domain. Rap1 activity regulated the junctional localization of KRIT-1 and its physical association with junction proteins. However, the association of the isolated KRIT-1 FERM domain was independent of Rap1. Small interfering RNA–mediated depletion of KRIT-1 blocked the ability of Rap1 to stabilize endothelial junctions associated with increased actin stress fibers. Thus, Rap1 increases KRIT-1 targeting to endothelial cell–cell junctions where it suppresses stress fibers and stabilizes junctional integrity.

Introduction

Cerebral cavernous malformations (CCMs) are vascular malformations mostly found within the central nervous system. CCMs can occur in sporadic or autosomal dominant inherited forms, the latter of which map to three loci, KRIT-1/CCM1, MGC4607/OSM/CCM2, and PDCD10/CCM3 (Dubovsky et al., 1995; Craig et al., 1998; Labauge et al., 2007; Liquori et al., 2007). KRIT-1 protein was detected in endothelial cells by Western blot, immunofluorescence, and immunohistochemistry (Gunel et al., 2002; Guzeloglu-Kayisli et al., 2004a,b), but this work was challenged because KRIT-1 mRNA was not detected in the endothelium (Petit et al., 2006). However, CCM lesions are composed of endothelial cells (Wong et al., 2000; Clatterbuck et al., 2001) and can occur outside the brain (Eerola et al., 2000). Furthermore, mice lacking KRIT-1 die because of defective vascular development but have apparently normal brain development (Whitehead et al., 2004), all of which suggest that the primary defect in CCM lesions is in the endothelial compartment.

KRIT-1 possesses four ankyrin repeats, a band 4.1/ezrin/radixin/moesin (FERM) domain, and multiple NPXY sequences, one of which is essential for integrin cytoplasmic domain-associated protein-1α (ICAP1α) binding (Zawistowski et al., 2002) and all of which mediate binding of CCM2 (Zawistowski et al., 2005; Zhang et al., 2007). KRIT-1 was identified as a Rap1-binding protein in yeast two hybrid experiments (Serebriiskii et al., 1997), and the FERM domain of KRIT-1 binds with 10-fold higher affinity to Rap1 than to H-Ras (Wohlgemuth et al., 2005). Although the interaction of Rap1 and full-length KRIT-1 has been disputed (Zhang et al., 2001), we have confirmed the association by coimmunoprecipitation (unpublished data). Rap1 regulates cell–cell junctions in both endothelial and epithelial cells (Knox and Brown, 2002; Price et al., 2004; Cullere et al., 2005). The disruption of endothelial cell junctions in CCM suggests that KRIT-1 may have a role in the capacity of Rap1 to regulate endothelial cell–cell junctions. Here, we report that KRIT-1 is expressed in endothelial cells where it is present in cell–cell junctions and associated with junctional proteins. The junctional localization of KRIT-1 is mediated by its FERM domain and regulated by Rap1 activity. Furthermore, we find that KRIT-1 is required for the stabilizing effect of Rap1 on endothelial cell–cell junctions. Together, these data establish that KRIT-1 is a Rap1-binding protein that regulates endothelial junction integrity and may provide a molecular explanation for aspects of the CCM phenotype.

A. Glading, J. Han, and R.A. Stockton contributed equally to this paper.

Dr. Han died on 4 July 2006.

Correspondence to M.H. Ginsberg: mhginsberg@ucsd.edu

Abbreviations used in this paper: 8-pCPT-2′-*O*-Me-cAMP, 8-pCPT-2′-*O*-methyl-adenosine-3′,5′-cAMP; BAEC, bovine aortic endothelial cell; CCM, cerebral cavernous malformation; CS, calf serum; FERM, band 4.1/ezrin/radixin/moesin; FN, fibronectin; GAP, GTPase activating protein; GAPDH, glyceraldehyde 3-phosphate dehydrogenase; HUVEC, human umbilical vein endothelial cell; ICAP1α, integrin cytoplasmic domain-associated protein-1α; NGS, normal goat serum.

The online version of this article contains supplemental material.

The Journal of Cell Biology, Vol. 179, No. 2, October 22, 2007 247–254
http://www.jcb.org/cgi/doi/10.1083/jcb.200705175

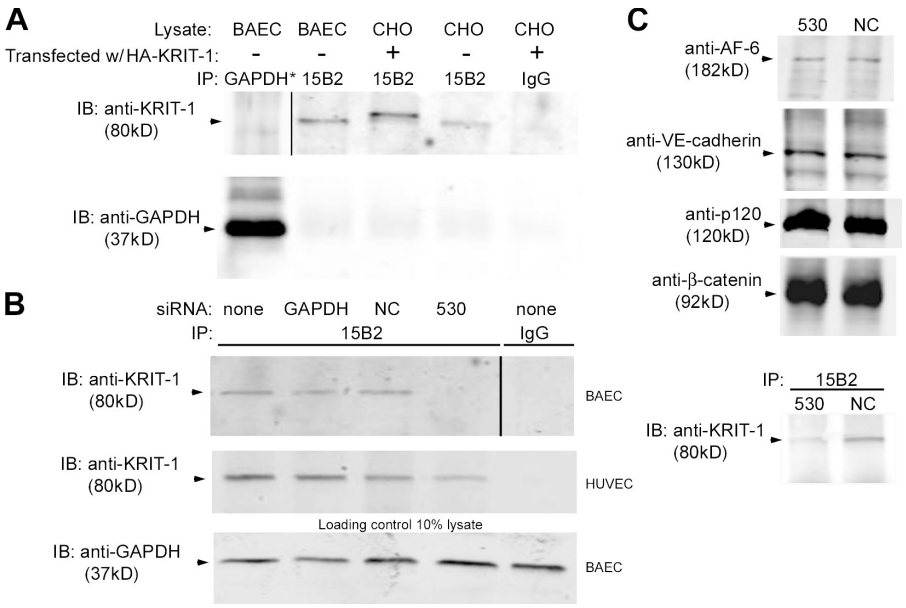

Figure 1. **Monoclonal anti–KRIT-1 (15B2) recognizes authentic KRIT-1 protein in endothelial cells.** (A) Immunoprecipitation using mAb anti–KRIT-1 (15B2) and immunoblotting with pAb anti–KRIT-1 (Rb6832) yields a band of ∼80 kD in endothelial and CHO cells. An irrelevant antibody, anti-GAPDH, and nonimmune mouse IgG did not immunoprecipitate the KRIT-1 band. Asterisk indicates that the input level of the lane was changed with Photoshop due to high background to show the absence of a band. (B) Antibody reactivity requires the presence of KRIT-1. siRNA against KRIT-1 (siRNA 530) eliminated the KRIT-1 band immunoprecipitated from BAECs and reduced that in HUVECs by 70%. Negative control siRNA and siRNA directed against GAPDH had no effect on KRIT-1 expression. Blots are representative; BAEC, $n = 3$; HUVEC, $n = 2$. (C) KRIT-1 depletion using anti–KRIT-1 siRNA 530 has no effect on the expression of junctional proteins. BAECs treated with anti–KRIT-1 siRNA (530) or control siRNA (NC) were Western blotted for junctional proteins. Although KRIT-1 knockdown of >80% was observed by immunoprecipitation and blotting of KRIT (bottom), no effect on the expression of junction proteins was seen. Blots are representative; $n = 3$. Black lines indicate that intervening lanes have been spliced out.

Results and discussion

Immunoprecipitation with an mAb anti–KRIT-1 (15B2) followed by Western blotting with an affinity-purified pAb (Rb6832) was performed to increase the sensitivity of detection of endogenous KRIT-1. We detected a band of ∼80 kD in bovine aortic endothelial cells (BAECs; Fig. 1, A and B) and human umbilical vein endothelial cells (HUVECs; Fig. 1 B). The mobility of this band is consistent with the calculated molecular mass of KRIT-1 (81 kD). Moreover, CHO cells also exhibited this 80-kD band, and when transfected with authentic HA-tagged human KRIT-1 exhibited a second intense band of slightly lower mobility consistent with the presence of the HA tag (Fig. 1 A). An unrelated antibody (glyceraldehyde 3-phosphate dehydrogenase [GAPDH]) did not immunoprecipitate KRIT-1, nor did nonimmune mouse IgG. We used siRNA-mediated knockdown of endogenous KRIT-1 to confirm that the endogenous 80-kD polypeptide was authentic KRIT-1. Transfection with KRIT-1–specific siRNA (530; Fig. 1 B) completely eliminated this band from BAECs and reduced it by 70% in HUVECs, but had no effect on the expression of a variety of cell–cell junction proteins (Fig. 1 C). An irrelevant (Fig. 1 C, GAPDH) and a negative control siRNA (NC) had no effect on the expression of this polypeptide.

Having shown the antibodies' specificity in immunoprecipitation blotting experiments, we then used the mAb anti–KRIT-1 to detect endothelial cell KRIT-1 by immunofluorescence. KRIT-1 staining was enriched at sites of cell–cell junctions and the nucleus in confluent bovine aortic endothelial monolayers (Fig. 2 A), but was absent from free membranes (not depicted), suggesting cell junction localization consistent with the reported localization of recombinant KRIT-1 in transfected HEK293 cells (Zawistowski et al., 2005). Staining specificity was confirmed by its marked reduction after transfection with the KRIT-1 siRNA 530 (Fig. 2 A). Similar staining was seen in HUVECs and was also observed with the affinity-purified pAb anti–KRIT-1. No staining was seen with nonimmune rabbit or mouse IgG (unpublished data). Thus, KRIT-1 protein is expressed in both arterial and venous endothelial cells in culture, which is consistent with its reported presence in endothelium in vivo (Guzeloglu-Kayisli et al., 2004a).

Confocal microscopy demonstrated that KRIT-1 staining was enriched in cell junctions and colocalized with β-catenin, a cell–cell junction protein (Fig. 2 A; Vestweber, 2000). In KRIT-1 siRNA 530–treated cells, β-catenin localization to the cell–cell junction was disrupted but global expression of junctional proteins was unchanged (Figs. 1 C and 2 A). β-catenin also physically associated with KRIT-1, as did p120-catenin and the junctional scaffold AF-6 (also called afadin; Miyahara et al., 2000), as judged by their presence in KRIT-1 immunoprecipitates (Fig. 2 B). The coimmunoprecipitation was done under conditions that garnered near complete recovery of KRIT-1 from the cell lysate. From this, we estimate that KRIT associates with ∼2% of total cellular β-catenin and p120-catenin and 6% of total AF-6. Nevertheless, the intensities of the KRIT-1 bands were similar to those observed for the junctional proteins, suggesting that KRIT-1 is not an abundant protein. This idea is supported by the requirement for prior immunoprecipitation to visualize KRIT-1 by immunoblotting (Fig. 2 B). The association of KRIT-1 with AF-6 is noteworthy as AF-6 can inhibit Rap1 activity (Su et al., 2003; Zhang et al., 2005) through recruitment of Rap GTPase activating proteins (GAPs). Thus, the interaction of KRIT-1 with AF-6 could act as a negative feedback modulator of Rap activity. Also present in coprecipitates, but not shown here, were vascular endothelial cadherin and α-catenin. In contrast, ZO-1, a tight junction marker, and talin, a focal adhesion protein absent from adherens junctions (Geiger et al., 1985), were not detected in KRIT-1 immunoprecipitates (Fig. 2 B).

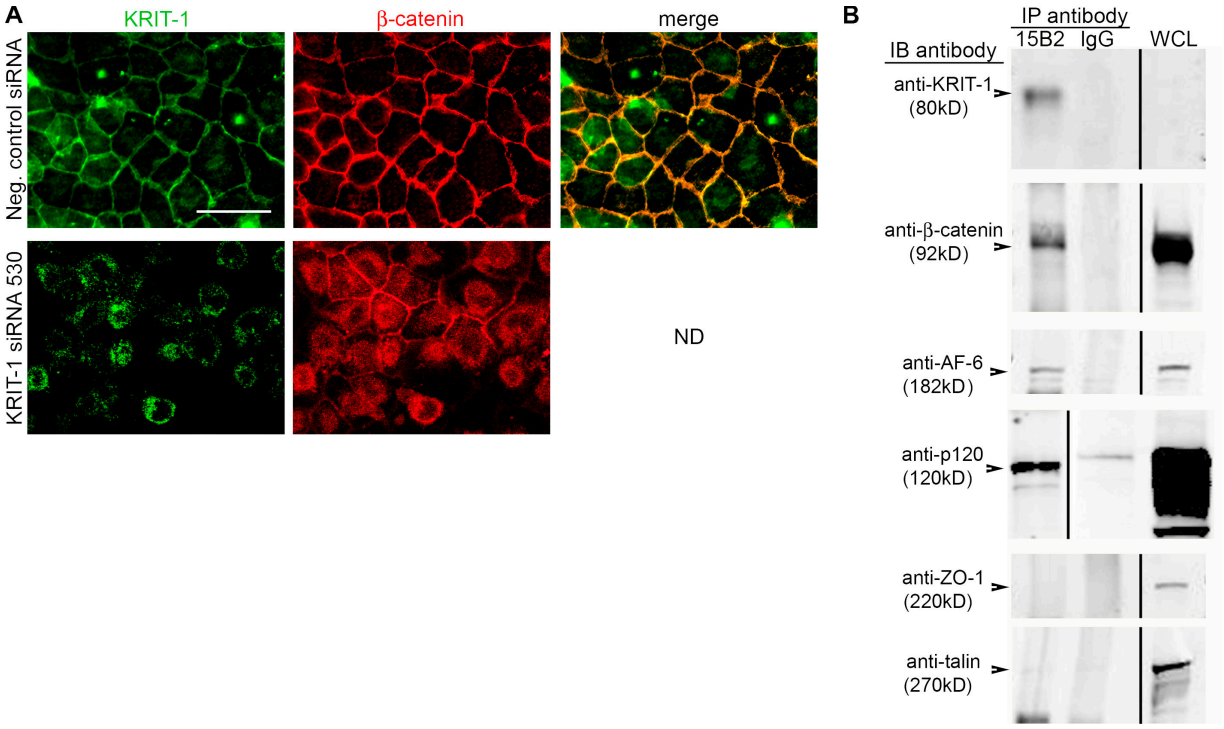

Figure 2. **KRIT-1 localizes to cell junctions and associates with junction proteins.** (A) KRIT-1 staining localizes to cell junctions (top left). mAb anti–KRIT-1 (15B2) recognizes endogenous KRIT-1 by immunofluorescence staining in untransfected and negative control siRNA–transfected BAECs (negative control siRNA–transfected cells are shown). Staining specificity was demonstrated by knockdown of KRIT-1 using siRNA 530 (bottom left). Confocal microscope images demonstrate a colocalization between KRIT-1 and β-catenin immunofluorescence (top right). In KRIT-1–depleted cells, β-catenin localization to the cell–cell junction is disrupted (bottom right). In top panels, the confocal imaging plane did not contain the nucleus, which does stain for KRIT-1 (not depicted); in bottom panels (with siRNA), the imaging plane slices through the nucleus. Confocal images are representative; $n = 3$. Bar, 50 μm. (B) KRIT-1 coimmunoprecipitates with β-catenin, AF-6, and p120-catenin but not with ZO-1 or talin. Lysates of BAECs were immunoprecipitated using monoclonal anti–KRIT-1 (15B2) or nonimmune mouse IgG (IgG). WCL, 10% of input whole cell lysate. Blots are representative; $n = 4$. All lanes were from the same membrane and black lines indicate that intervening lanes have been spliced out, or in the case of the p120 blot, reordered for clarity.

KRIT-1 associates with Rap1 small GTPase and exhibits a preference for Rap versus Ras in vitro (Serebriiskii et al., 1997; Wohlgemuth et al., 2005). We therefore asked whether Rap1 could regulate the localization of KRIT-1 to the junctions and its association with junctional proteins. Transfection of cells with an activated Rap1 (Rap1A-G12V, referred to as RapV12) increased the association of endogenous KRIT-1 with β-catenin and AF-6 (Fig. 3 A). Expression of the inhibitor of Rap activity (Rap1GAP) inhibited the association of KRIT-1 with β-catenin and AF-6 to a greater extent than the increase elicited by activated Rap1A. The strong effect of Rap1GAP suggests the presence of basal Rap activity in BAECs. Neither RapV12 nor Rap1GAP expression affected KRIT-1 expression (Fig. 3 A). Furthermore, thrombin treatment led to a dramatic loss of KRIT-1 from the junctions (Fig. 3 B) but did not alter KRIT-1 expression (Fig. S1 A, available at http://www.jcb.org/cgi/content/full/200705175/DC1). Thrombin's effect was counteracted by the addition of an activator (Enserink et al., 2002) of the RapGEF Epac-1, 8-pCPT-2′-*O*-methyladenosine-3′,5′-cAMP (8-pCPT-2′-*O*-Me-cAMP; Fig. 3 B) . RapV12 also reversed the thrombin-stimulated loss of KRIT from the junctions, supporting the idea that effect of 8-pCPT-2′-*O*-Me-cAMP is caused by the activation of Rap1 and that KRIT-1 association with cell–cell junctions is increased by Rap1 activation.

To explore the mechanism of KRIT-1 targeting of endothelial cell–cell junctions, we examined the capacity of different domains of the protein to mediate junctional localization. The isolated KRIT-1 FERM domain (GFP-KRIT-F123; Fig. 4 A) colocalized with β-catenin in cell–cell junctions (Fig. 4 B). Furthermore, the KRIT-1 FERM domain was physically associated with β-catenin (Fig. 4 C). In sharp contrast to the intact protein, the interaction of GFP-KRIT-F123 with β-catenin was insensitive to the activation state of Rap1 (Fig. 4 D), suggesting that active Rap1 may increase the association of KRIT-1 with junctional proteins by increasing the availability of this domain. In contrast to the FERM domain, the KRIT-1 N terminus (Fig. 4 A) did not colocalize with either junctional β-catenin (Fig. 4 B) or ZO-1. Furthermore, the N terminus did not associate with β-catenin in coimmunoprecipitation experiments (Fig. 4 C). Moreover, the KRIT-F23 fragment of the FERM domain failed to localize to junctions, suggesting that the F1 region is required for localization to the junction. Thus, KRIT-1 localization to endothelial junctions is mediated by the KRIT-1 FERM domain and regulated by Rap1.

CCM lesions display characteristics typical of a loss of endothelial cell–cell junctions (Clatterbuck et al., 2001). As noted previously, KRIT-1 is a relatively specific Rap1 effector (Serebriiskii et al., 1997; Wohlgemuth et al., 2005), and Rap1 regulates the integrity of cell–cell junctions in endothelial and epithelial cells (Knox and Brown, 2002; Price et al., 2004; Cullere et al., 2005), leading us to examine the role of KRIT-1 in

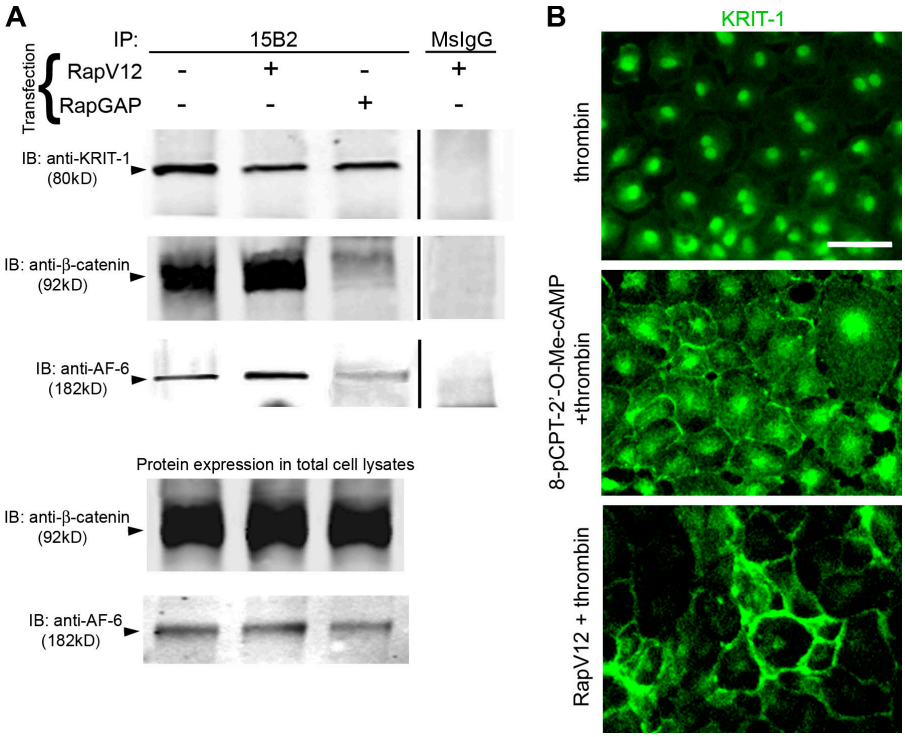

Figure 3. **KRIT-1 is a Rap1 effector protein and Rap1 regulates KRIT-1 junctional association.** (A) Expression of RapV12 increases coimmunoprecipitation of β-catenin and AF-6 with KRIT-1, whereas expression of Rap1GAP reduces association. Transfection of BAECs with RapV12 or Rap1GAP does not affect the expression of KRIT-1 (top) or β-catenin and AF-6 as shown by Western blot of input lysate (bottom). Black lines indicate that intervening lanes have been spliced out; all lanes were cut from the same membrane. Blots are representative; $n = 4$. (B) Rap1 activation counteracts thrombin-mediated reduction of junctional KRIT-1. 2 U/ml thrombin treatment reduced KRIT-1 localization to cell–cell junctions. Treatment with 8-pCPT-2′-*O*-Me-cAMP before thrombin treatment prevented the loss of KRIT-1 from junctions. KRIT-1 localization in BAECs transfected with RapV12 was relatively resistant to thrombin treatment. Confocal images are representative; $n = 3$. Bar, 50 μm.

Rap1-induced stabilization of endothelial junctions. We noted that there was extensive redistribution of β-catenin out of cell–cell junctions in KRIT-1–depleted BAECs (Fig. 1 A), suggesting that KRIT-1 might be required for the stability of cell–cell junctions in these cells. As a test for the function of these junctions, we examined the permeability of endothelial cell monolayers to HRP (Stockton et al., 2004). KRIT-1 siRNA transfection caused an approximately twofold increase in permeability (Fig. 5 A) that was reversed by reconstitution with recombinant KRIT-1. Furthermore, treatment of KRIT-1–depleted cells with 8-pCPT-2′-*O*-Me-cAMP had little effect on permeability (Fig. 5 A). In sharp contrast, 8-pCPT-2′-*O*-Me-cAMP reversed the increase in permeability caused by thrombin as expected (Rangarajan et al., 2003; Cullere et al., 2005). Thrombin treatment caused a loss of KRIT-1 from the junctions (Fig. 3 B) and a concomitant redistribution of β-catenin away from the junction (Fig. S1 B); however, thrombin treatment did not disrupt the interaction of KRIT-1 and β-catenin, suggesting that they remain associated as they redistribute away from the junction (Fig. S1 A). Thrombin increased permeability further in KRIT-1–depleted cells. Furthermore, overexpression of KRIT-1 partially reversed the increased permeability induced by expression of Rap1GAP (Fig. 5 B). Thus, KRIT-1 regulates endothelial permeability and is required for Rap1-mediated stabilization of endothelial junctions.

We have shown here that Rap1 activation leads to association of KRIT-1 with endothelial cell–cell junction proteins. The KRIT-1 N terminus has binding sites for ICAP1α and CCM2 (Zawistowski et al., 2002, 2005; Zhang et al., 2007). Consequently, recruitment of KRIT-1 through its FERM domain has the potential to bring these proteins to the junction. Both ICAP1α and CCM2 are involved in the regulation of Rho family GTPases (Degani et al., 2002; Zawistowski et al., 2005), which are known to control the integrity of endothelial junctions via the actin cytoskeleton (Wojciak-Stothard and Ridley, 2002). Furthermore, activation of Rap1 by 8-pCPT-2′-*O*-Me-cAMP inhibits thrombin-induced RhoA activation in endothelial cells (Cullere et al., 2005). Hence, we examined F-actin distribution after depletion of KRIT-1 with siRNA. In control cells, actin was distributed around the circumference of each cell, and few stress fibers were observed. This contrasts strongly with KRIT-1 siRNA–treated cells, which had abundant stress fibers. Overexpression of HA-KRIT in control cells increased cortical actin staining, and HA-KRIT reexpression restored cortical actin morphology in KRIT-1 siRNA–treated cells (Fig. 5 C). As changes in actin morphology are linked to altered permeability (Stockton et al., 2004; Kooistra et al., 2005; Hayashi et al., 2006), this result suggests that KRIT-1 may act as a scaffold that regulates endothelial junctions by recruiting modulators of the Rho family GTPases that control the actin cytoskeleton.

CCM lesions are composed of a bed of leaky capillaries (Wong et al., 2000; Clatterbuck et al., 2001). Thus, our finding that the loss of KRIT-1 increases endothelial permeability provides a direct link between the pathogenesis of CCM and KRIT-1 function. KRIT-1 is a relatively specific effector of Rap1, which is a regulator of endothelial permeability and the stability of cell–cell junctions (Knox and Brown, 2002; Cullere et al., 2005). We now find that the capacity of Rap1 to stabilize endothelial cell junctions depends on KRIT-1 and that Rap1 regulates the junctional localization of the KRIT-1 protein and increases the association of KRIT-1 with junctional proteins. The KRIT-1 FERM domain mediates its association with junctional proteins and the isolated FERM domain associates with junctional proteins in a Rap1-independent manner. This suggests that the

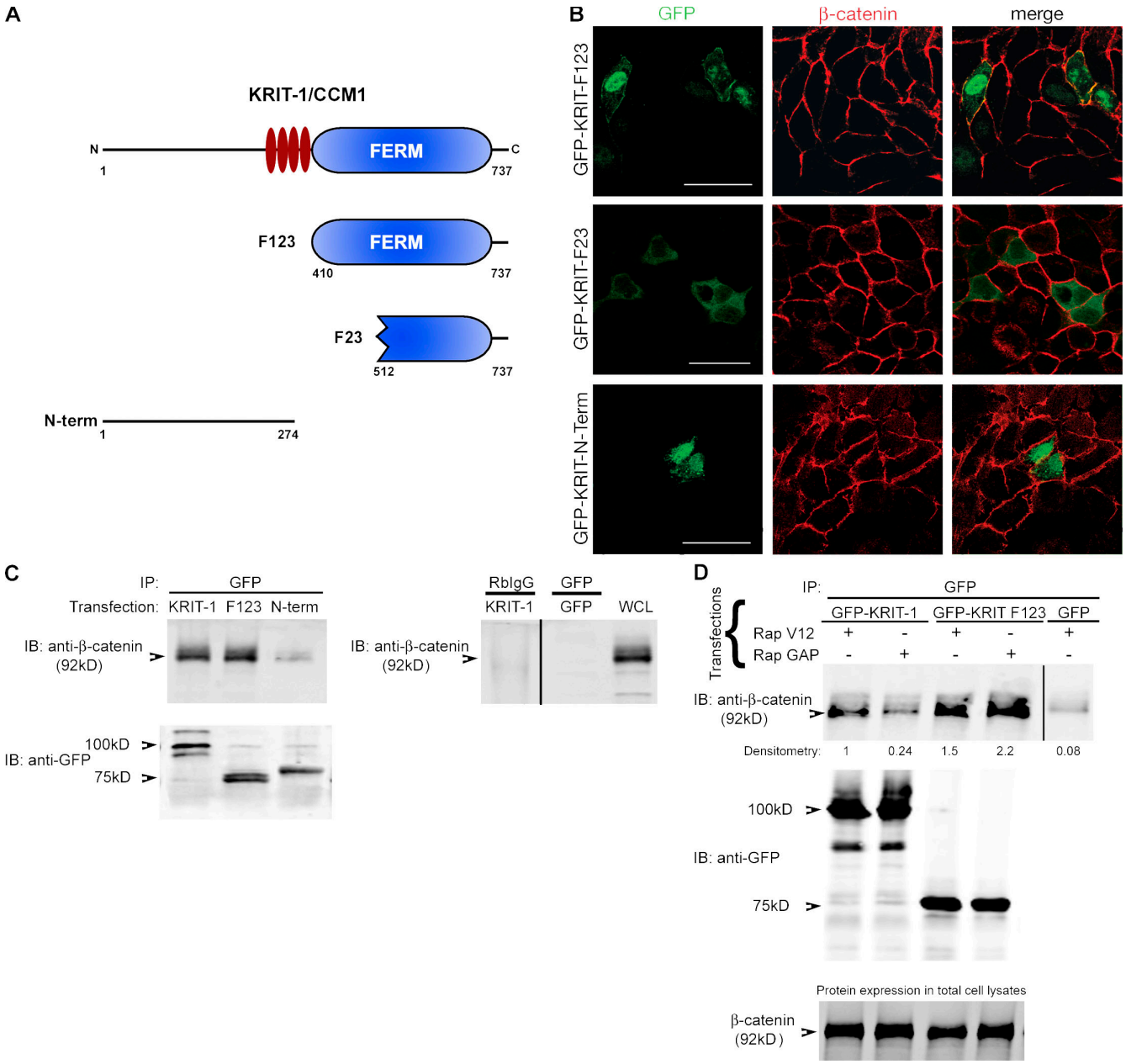

Figure 4. **KRIT-1 junctional localization is regulated by Rap1 and requires the FERM domain.** (A) Schematic of KRIT-1 constructs. All constructs include an N-terminal GFP tag not depicted here. (B) GFP-tagged KRIT-1 FERM domain (GFP-KRIT-F123) colocalized with β-catenin in bovine aortic endothelial cell–cell junctions. A KRIT-1 FERM domain truncation (GFP-F23) does not localize to cell junctions nor does a KRIT-1 N-terminal construct containing the ICAP1α and CCM2 binding sites. Minor colocalization with β-catenin is seen in the cytoplasm of all treatments. Confocal images are representative; $n = 5$. Bars, 50 μm. (C) Full-length GFP–KRIT-1 (KRIT-1) and GFP-KRIT-F123 (F123) coimmunoprecipitate with β-catenin, whereas the GFP-labeled N terminus (N-term) does not. BAECs expressing GFP-labeled KRIT-1 constructs were immunoprecipitated with rabbit anti-GFP and blotted with anti–β-catenin (left). Blotting with mouse anti-GFP demonstrated similar expression of each construct. GFP alone did not coimmunoprecipitate β-catenin, nor did immunoprecipitation with nonimmune rabbit IgG of lysates of cells transfected with GFP–KRIT-1 (right). 10% of input lysate (WCL) from GFP-KRIT-F123–transfected cells was blotted to assess expression of β-catenin. Lanes were cut from the same membrane and reordered using Photoshop. (D) Association of GFP-KRIT-F123 and β-catenin is insensitive to Rap1 activation. BAECs were transfected with GFP–KRIT-1, GFP-KRIT-F123, or GFP alone in the presence of either RapV12 or RapGAP. Anti-GFP immunoprecipitates were immunoblotted for β-catenin. Rap1GAP reduced the association of full-length KRIT-1with β-catenin ~75% (as evaluated by densitometry). This decrease was not seen in precipitates from GFP-KRIT-F123–expressing cells (top). In parallel, anti-GFP immunoprecipitates were blotted with mouse anti-GFP and 10% of input lysate was blotted for β-catenin to assess expression of the interacting proteins (bottom). Blots are representative; $n = 3$. Black lines indicate that intervening lanes have been spliced out.

availability of the KRIT-1 FERM domain may be regulated by the binding of active Rap1. This would allow KRIT-1 to associate via the FERM domain with the junction complex, thus stabilizing cell–cell junctions, perhaps through modifying the activity of Rho family GTPases. In summary, Rap1 stimulates the junctional localization of KRIT-1 via KRIT-1's FERM domain, and KRIT-1 is required for Rap1 stabilization of endothelial junctions. These data provide a molecular linkage between KRIT-1 protein function and the CCM phenotype and identify a Rap effector that regulates cell–cell junctions.

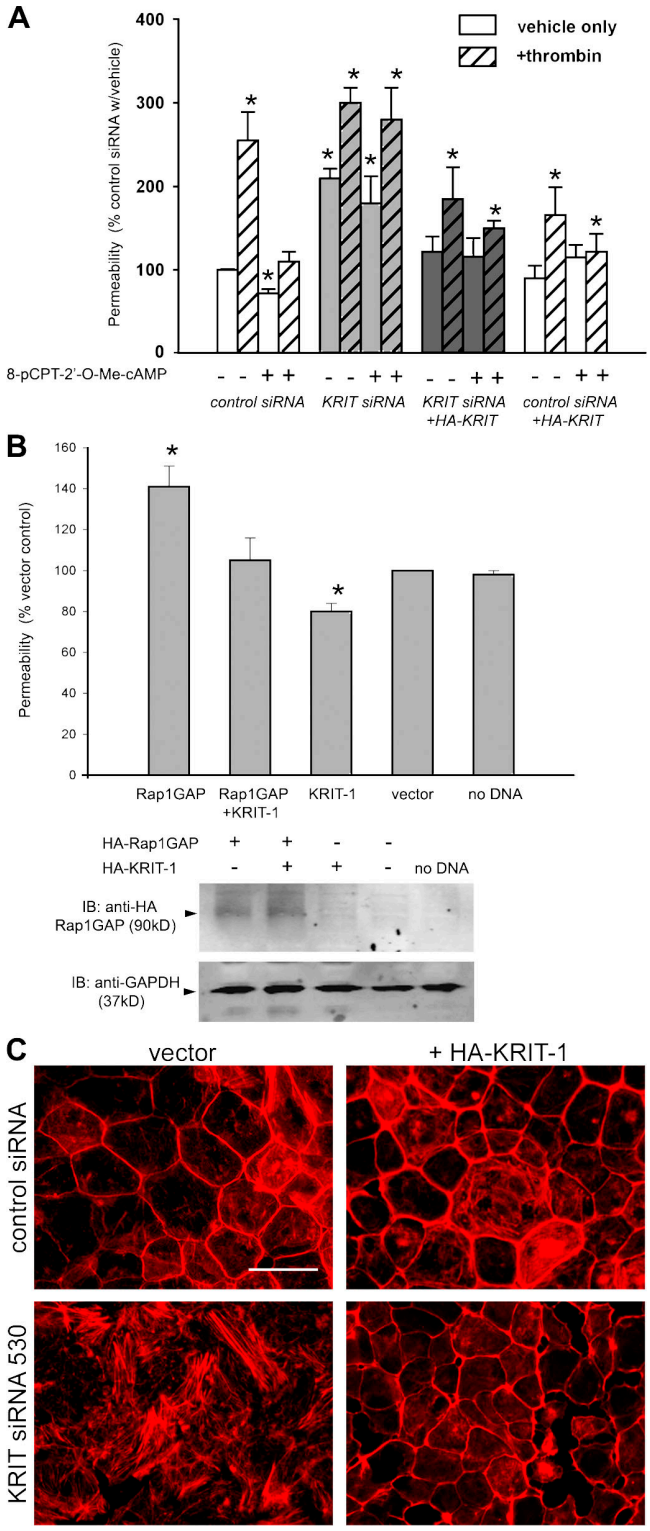

Figure 5. **KRIT-1 regulates endothelial cell permeability.** (A) Treatment of BAECs with 2 U/ml thrombin increased endothelial permeability to HRP, whereas treatment with 8-pCPT-2′-*O*-Me-cAMP inhibited thrombin-stimulated permeability, as did overexpression of recombinant KRIT-1 (in control siRNA–treated cells). Knockdown of KRIT-1 expression by KRIT-1 siRNA 530 caused an approximately twofold increase in permeability. Thrombin treatment further increased permeability in KRIT-1–depleted cells. However, 8-pCPT-2′-*O*-Me-cAMP had little effect on permeability in these cells. The increased permeability was almost completely rescued by reexpression of recombinant KRIT-1. Negative control siRNA had no effect on permeability. Data shown is the mean increase in permeability ± SEM; $n = 5$. *, $P < 0.05$ compared with control siRNA plus vehicle. (B) KRIT-1 overexpression reverses Rap1GAP-induced increased endothelial permeability. Data shown is the mean increase in permeability ± SEM; $n = 4$. *, $P < 0.05$ compared with vector control. (bottom) A representative blot of Rap1GAP expression in the cells used for permeability experiments. (C) Depletion of KRIT-1 increases stress fiber formation. The actin cytoskeleton of anti–KRIT-1 siRNA–treated and HA–KRIT-1–reconstituted cells was stained with rhodamine-phalloidin to assess changes in the distribution of F-actin as a consequence of KRIT-1 depletion. Epifluorescence images are representative; $n = 3$. Bar, 50 μm.

Materials and methods

Cell culture

BAECs were a gift of S. Shattil (University of California, San Diego, La Jolla, CA). BAECs were cultured in DME with 10% calf serum (CS) and 1% penicillin/streptomycin (Invitrogen). HUVECs were obtained from Cambrex and cultured in endothelial growth medium 2 (Cambrex). CHO cells were obtained from American Type Culture Collection. CHO cells were cultured in DME with 10% fetal bovine serum plus 1% penicillin/streptomycin, 1% L-glutamine, and 1% nonessential amino acids (Invitrogen).

siRNA and cDNA

siRNA directed against human KRIT was designed by Ambion. Three predesigned siRNA sequences (146530, 146531, and 214883) were tested and all were found to inhibit expression of KRIT protein in human cells. siRNA 146530 (530) was found to have activity in BAECs, as would be expected from its 100% identity in the target sequence, and was used in all subsequent experiments. Control siRNA was obtained from Ambion, including anti-GAPDH and negative control siRNA 1. All siRNA was used at equimolar concentrations.

cDNA encoding HA- and GFP-tagged full-length KRIT, a GFP-tagged KRIT FERM domain (GFP-F123), and a GFP-tagged FERM domain truncation (GFP-F23) was constructed from full-length KRIT-1 cDNA provided by H. Dietz (Johns Hopkins University, Baltimore, MD). Domain boundaries were estimated using protein sequence alignment with other FERM-containing proteins: KRIT-1 FERM (F123) extended from amino acids 410–737, F23 amino acids 512–737, and KRIT-1 N terminus amino acids 1–274. A GFP-tagged N-terminal truncation of KRIT was made by subcloning the N terminus from a GST construct into the pEGFP-C1 vector (CLONTECH Laboratories, Inc.). Mammalian expression constructs for HA-Rap1A-G12V (RapV12) and HA-Rap1GAP (RapGAP) were gifts from J. Bos (Utrecht University, Utrecht, Netherlands).

Transfection

CHO cells were transfected with Lipofectamine Plus (Invitrogen) according to the manufacturer's instructions. Cells were plated at 80% confluence 24 h before transfection and media was replaced 3 h after transfection.

For Western blot detection of siRNA efficiency, siRNA was transfected into BAECs and HUVECs using HiPerfect transfection reagent (QIAGEN) according to the manufacturer's suggested instructions. Cells were plated at 60–70% confluence and 25 nM siRNA was incubated with the cells for 24–48 h with no difference in knockdown efficiency.

For permeability, immunofluorescence, and cotransfection studies, BAECs were transfected using a nucleofection device (Amaxa). In brief, 0.5×10^6 cells per transfection were suspended in Basic endothelial cell solution (Amaxa) together with 25 nM siRNA with or without 1 μg DNA. The cells were then nucleoporated using program M-003 (Amaxa). After recovery at 37°C for 10 min, the cells were plated as required. This method garnered transfection efficiencies from 70 to 90%.

Anti–KRIT-1 antibody production and characterization

Polyclonal anti–KRIT-1 6832 was developed against the recombinant KRIT-1 FERM (F123) domain coupled to keyhole limpet hemocyanin. Monoclonal anti–KRIT-1 antibodies were also developed using the recombinant KRIT-1 FERM (F123) domain as the antigen. Mice were immunized with the KRIT-1 FERM domain in incomplete Freund's adjuvant. Mouse sera were titered by ELISA against GST-F123 before fusion of splenic cells with myeloma cells. After fusion, single hybridoma cells were plated by limiting dilution, and antibody production was assayed in the hybridoma supernatant by ELISA. Titers were done in parallel on GST-coated plates to assess background binding. Hybridomas with high titer were selected for subcloning, and the process was repeated twice. Selected hybridoma supernatants were further purified by affinity chromatography on a protein G–Sepharose column.

Immunoprecipitation and Western blotting

For endogenous coimmunoprecipitation experiments, cells expressing KRIT-1 were scraped into 500 μl of lysis buffer containing 50 mM Tris, pH 7.4, 150 mM NaCl, 0.5% NP-40, and 5 mM $MgCl_2$ plus a protease inhibitor cocktail (Roche). After resting 5 min on ice, the lysate was incubated for 15 min at 4°C with rocking. The lysate was spun down at 14,000 rpm for 10 min and the protein concentration of the supernatant was determined using a bicinchoninic acid assay (Pierce Chemical Co.). 500 μg of precleared total cell protein was added to 2 μg of immunoprecipitating antibody and incubated at 4°C with continuous rocking for 2 h. 10 μl of a 50% slurry of protein G–Sepharose beads (GE Healthcare) was then added and the rocking of the samples was continued overnight. The immunoprecipitated samples were washed three times with lysis buffer and solubilized with 10 μl SDS-PAGE sample buffer. Samples were resolved on 4–20% polyacrylamide gels (Invitrogen) in SDS-PAGE buffer and transferred to nitrocellulose membranes.

Anti–KRIT-1 15B2 was used for immunofluorescence at a dilution of 1:1,000. Rabbit anti-GFP (Invitrogen) was used at a dilution of 1:200 for immunoprecipitation of GFP-tagged proteins. Nonimmune mouse IgG was obtained from Santa Cruz Biotechnology, Inc. Rabbit anti–human–KRIT-1 6832 serum was used for immunoblotting at a dilution of 1:1,000. Mouse anti–human AF-6 (BD Biosciences), mouse anti–human ZO-1 (Zymed Laboratories), rabbit anti–human VE-cadherin (CD144; Serotec), mouse anti-murine p120-catenin (Sigma-Aldrich), and rabbit anti–human GAPDH (Santa Cruz Biotechnology, Inc.) were used for immunoblotting at dilutions of 1:1,000. Mouse anti–chicken β-catenin (6F9; Sigma-Aldrich), mouse anti-GFP (Invitrogen), and mouse anti–chicken talin (8d4; Sigma-Aldrich) were used for immunoblotting at dilutions of 1:5,000, 1:2,500, and 1:3,000, respectively. Anti–β-catenin was used in immunofluorescence at a dilution of 1:1,000. Blots were probed with the appropriate secondary antibody conjugated to Alexa 680 (Invitrogen) or IRDye 800 (Rockland Immunochemicals) and imaged using an infrared imaging system (Odyssey; Li-Cor). Blots were processed using Photoshop (Adobe) and all lanes were adjusted equally.

Immunofluorescence

BAECs were grown to confluence on fibronectin (FN)-coated glass coverslips. Slips were fixed with 4% formaldehyde for 20 min, permeabilized for 10 min with 0.2% Triton X-100 (Sigma-Aldrich), and blocked for 1 h with 10% normal goat serum (NGS; Sigma-Aldrich) in PBS. Anti–β-catenin (1:1,000 in NGS) was added and incubated at RT for 1 h in a humidified chamber. Slips were washed three times with PBS plus 0.001% Triton X-100 (PBS-TX100), and then goat anti–mouse IgG Alexa 568, goat anti–mouse IgG Alexa 488, or goat anti–rabbit IgG Alexa 568 (Invitrogen) in NGS was added at 1:1,000 and incubated for 1 h at RT. Control stain was performed with second antibody only at 1:1,000. Slips were washed six times in PBS-TX100 and mounted on glass slides using 10 μl of fluorescent mounting medium (DakoCytomation) and dried overnight. Images were obtained using a confocal microscopy system (TCS SP2 AOBS; Leica DMRE microscope with an HCX PL APO 63× 1.32 oil objective). Images were processed using Photoshop. Colocalization images were created using ImageJ software (National Institutes of Health).

Concomitant to the leak assay, a portion of the transfected cells was plated on FN-coated glass coverslips and grown to confluence (~24 h) in low-glucose DME/10% CS. Cells were serum starved (0.5% CS) for 4 h then treated for 30 min with 100 μM 8-pCPT-2′-*O*-Me-cAMP or the vehicle alone (control), and indicated cells were treated with 2 U/ml thrombin for 60 min. Slips were fixed with 3.5% formaldehyde for 2 h, permeabilized for 10 min with 0.15% Triton X-100 and washed with TBST. Slips were blocked with 10% NGS for 60 min at RT and washed again. 200 μl/slip of primary antibody was incubated overnight at 4°C in a humidified chamber. The control stain was mouse IgG at 1:1,000. After washing, donkey anti–mouse IgG Alexa 488 (Invitrogen) was added at a 1:1,000 dilution overnight at 4°C. Coverslips were washed six times in alternating PBS/TBST rinses and mounted on 10 μl Prolong Gold mounting medium (Invitrogen) and photographed using a confocal microscopy system. Images were processed using Photoshop. For actin staining (Fig. 5 C), cells were incubated with a 1:200 dilution of Alexa 488 or Alexa 568–phalloidin (6 μM in methanol; Invitrogen) overnight at 4°C. Coverslips were washed and mounted as above and imaged using a microscope (DMLS; Lecia NPlan 40× 0.65 objective) with a camera (SPOT RT Color-2000; Diagnostic Instruments).

BAEC monolayer leak assay

The permeability of the endothelial monolayer was evaluated using a leak assay originally described in Stockton et al. (2004). In brief, BAECs were grown to semiconfluence. Cells were transfected with 25 nM of negative control siRNA or KRIT-1 siRNA 530 with or without 1 μg pcDNA3.1 HA–KRIT-1. Transfected cells in phenol-free DME/10% CS were plated into 3-μm-pore polyester FN-coated transwell filters (Corning). Filter-plated cells were incubated for 48 h at 37°C to full confluence. Cells were then incubated in serum-free, phenol-free DME for 2 h. As indicated in the figure legends, in some conditions cells were treated with 100 μM 8-pCPT-2′-*O*-Me-cAMP for 30 min, and then half were treated with 2 U/ml thrombin (GE Healthcare) for 30 min. 50 μl of phenol-free DME containing 1.5 μg/ml HRP (Sigma-Aldrich) was added to upper wells for an additional 30 min. Filters were removed from outer wells and fixed in 3.5% formaldehyde and later stained with 0.25% Coomassie blue and examined by phase-contrast microscopy to reconfirm the integrity of cell monolayers.

The HRP content of the lower chamber medium was measured using a microplate peroxidase colorimetric assay. 100-μl-per-well guaiacol/sodium phosphate assay buffer (1:1) was added to 25 μl of each sample in triplicate. 25 μl of freshly made 0.6-mM H_2O_2 in ddH_2O was added to each well for ~15 min or until color developed. Reaction was stopped with 10-μl-per-well 2N H_2SO_4. A_{490} was acquired and raw absorbance values were normalized as a percentage of control untransfected (vehicle) cell sample absorbance. Data was analyzed for statistical significance using analysis of variance and SigmaStat software (Jandel).

Online supplemental material

Fig. S1 shows the effect of thrombin treatment on KRIT-1 expression, association with β-catenin, and β-catenin localization. Online supplemental material is available at http://www.jcb.org/cgi/content/full/200705175/DC1.

This work was supported by grants from the National Institutes of Health (AR27214, HL 078784, and HL31950). A. Glading is a postdoctoral fellow of the American Cancer Society and J. Han was an arthritis investigator of the Arthritis Foundation.

Submitted: 29 May 2007
Accepted: 19 September 2007

References

Clatterbuck, R.E., C.G. Eberhart, B.J. Crain, and D. Rigamonti. 2001. Ultrastructural and immunocytochemical evidence that an incompetent blood-brain barrier is related to the pathophysiology of cavernous malformations. *J. Neurol. Neurosurg. Psychiatry*. 71:188–192.

Craig, H.D., M. Gunel, O. Cepeda, E.W. Johnson, L. Ptacek, G.K. Steinberg, C.S. Ogilvy, M.J. Berg, S.C. Crawford, R.M. Scott, et al. 1998. Multilocus linkage identifies two new loci for a mendelian form of stroke, cerebral cavernous malformation, at 7p15-13 and 3q25.2-27. *Hum. Mol. Genet.* 7:1851–1858.

Cullere, X., S.K. Shaw, L. Andersson, J. Hirahashi, F.W. Luscinskas, and T.N. Mayadas. 2005. Regulation of vascular endothelial barrier function by Epac, a cAMP-activated exchange factor for Rap GTPase. *Blood*. 105:1950–1955.

Degani, S., F. Balzac, M. Brancaccio, S. Guazzone, S.F. Retta, L. Silengo, A. Eva, and G. Tarone. 2002. The integrin cytoplasmic domain-associated protein ICAP-1 binds and regulates Rho family GTPases during cell spreading. *J. Cell Biol.* 156:377–387.

Dubovsky, J., J.M. Zabramski, J. Kurth, R.F. Spetzler, S.S. Rich, H.T. Orr, and J.L. Weber. 1995. A gene responsible for cavernous malformations of the brain maps to chromosome 7q. *Hum. Mol. Genet.* 4:453–458.

Eerola, I., K.H. Plate, R. Spiegel, L.M. Boon, J.B. Mulliken, and M. Vikkula. 2000. KRIT1 is mutated in hyperkeratotic cutaneous capillary-venous malformation associated with cerebral capillary malformation. *Hum. Mol. Genet.* 9:1351–1355.

Enserink, J.M., A.E. Christensen, J. de Rooij, M. van Triest, F. Schwede, H.G. Genieser, S.O. Doskeland, J.L. Blank, and J.L. Bos. 2002. A novel Epac-specific cAMP analogue demonstrates independent regulation of Rap1 and ERK. *Nat. Cell Biol.* 4:901–906.

Geiger, B., T. Volk, and T. Volberg. 1985. Molecular heterogeneity of adherens junctions. *J. Cell Biol.* 101:1523–1531.

Gunel, M., M.S. Laurans, D. Shin, M.L. DiLuna, J. Voorhees, K. Choate, C. Nelson-Williams, and R.P. Lifton. 2002. KRIT1, a gene mutated in cerebral cavernous malformation, encodes a microtubule-associated protein. *Proc. Natl. Acad. Sci. USA*. 99:10677–10682.

Guzeloglu-Kayisli, O., N.M. Amankulor, J. Voorhees, G. Luleci, R.P. Lifton, and M. Gunel. 2004a. KRIT1/cerebral cavernous malformation 1 protein localizes to vascular endothelium, astrocytes, and pyramidal cells of the adult human cerebral cortex. *Neurosurgery*. 54:943–949 (discussion 949).

Guzeloglu-Kayisli, O., U.A. Kayisli, N.M. Amankulor, J.R. Voorhees, O. Gokce, M.L. DiLuna, M.S. Laurans, G. Luleci, and M. Gunel. 2004b. Krev1 interaction trapped-1/cerebral cavernous malformation-1 protein expression during early angiogenesis. *J. Neurosurg.* 100:481–487.

Hayashi, S., K. Takeuchi, S. Suzuki, T. Tsunoda, C. Tanaka, and Y. Majima. 2006. Effect of thrombin on permeability of human epithelial cell monolayers. *Pharmacology*. 76:46–52.

Knox, A.L., and N.H. Brown. 2002. Rap1 GTPase regulation of adherens junction positioning and cell adhesion. *Science*. 295:1285–1288.

Kooistra, M.R., M. Corada, E. Dejana, and J.L. Bos. 2005. Epac1 regulates integrity of endothelial cell junctions through VE-cadherin. *FEBS Lett.* 579:4966–4972.

Labauge, P., C. Denier, F. Bergametti, and E. Tournier-Lasserve. 2007. Genetics of cavernous angiomas. *Lancet Neurol.* 6:237–244.

Liquori, C.L., M.J. Berg, F. Squitieri, T.P. Leedom, L. Ptacek, E.W. Johnson, and D.A. Marchuk. 2007. Deletions in CCM2 are a common cause of cerebral cavernous malformations. *Am. J. Hum. Genet.* 80:69–75.

Miyahara, M., H. Nakanishi, K. Takahashi, K. Satoh-Horikawa, K. Tachibana, and Y. Takai. 2000. Interaction of nectin with afadin is necessary for its clustering at cell-cell contact sites but not for its cis dimerization or trans interaction. *J. Biol. Chem.* 275:613–618.

Petit, N., A. Blecon, C. Denier, and E. Tournier-Lasserve. 2006. Patterns of expression of the three cerebral cavernous malformation (CCM) genes during embryonic and postnatal brain development. *Gene Expr. Patterns*. 6:495–503.

Price, L.S., A. Hajdo-Milasinovic, J. Zhao, F.J. Zwartkruis, J.G. Collard, and J.L. Bos. 2004. Rap1 regulates E-cadherin-mediated cell-cell adhesion. *J. Biol. Chem.* 279:35127–35132.

Rangarajan, S., J.M. Enserink, H.B. Kuiperij, J. de Rooij, L.S. Price, F. Schwede, and J.L. Bos. 2003. Cyclic AMP induces integrin-mediated cell adhesion through Epac and Rap1 upon stimulation of the β_2-adrenergic receptor. *J. Cell Biol.* 160:487–493.

Serebriiskii, I., J. Estojak, G. Sonoda, J.R. Testa, and E.A. Golemis. 1997. Association of Krev-1/rap1a with Krit1, a novel ankyrin repeat-containing protein encoded by a gene mapping to 7q21-22. *Oncogene*. 15:1043–1049.

Stockton, R.A., E. Schaefer, and M.A. Schwartz. 2004. p21-activated kinase regulates endothelial permeability through modulation of contractility. *J. Biol. Chem.* 279:46621–46630.

Su, L., M. Hattori, M. Moriyama, N. Murata, M. Harazaki, K. Kaibuchi, and N. Minato. 2003. AF-6 controls integrin-mediated cell adhesion by regulating Rap1 activation through the specific recruitment of Rap1GTP and SPA-1. *J. Biol. Chem.* 278:15232–15238.

Vestweber, D. 2000. Molecular mechanisms that control endothelial cell contacts. *J. Pathol.* 190:281–291.

Whitehead, K.J., N.W. Plummer, J.A. Adams, D.A. Marchuk, and D.Y. Li. 2004. Ccm1 is required for arterial morphogenesis: implications for the etiology of human cavernous malformations. *Development*. 131:1437–1448.

Wohlgemuth, S., C. Kiel, A. Kramer, L. Serrano, F. Wittinghofer, and C. Herrmann. 2005. Recognizing and defining true Ras binding domains I: biochemical analysis. *J. Mol. Biol.* 348:741–758.

Wojciak-Stothard, B., and A.J. Ridley. 2002. Rho GTPases and the regulation of endothelial permeability. *Vascul. Pharmacol.* 39:187–199.

Wong, J.H., I.A. Awad, and J.H. Kim. 2000. Ultrastructural pathological features of cerebrovascular malformations: a preliminary report. *Neurosurgery*. 46:1454–1459.

Zawistowski, J.S., I.G. Serebriiskii, M.F. Lee, E.A. Golemis, and D.A. Marchuk. 2002. KRIT1 association with the integrin-binding protein ICAP-1: a new direction in the elucidation of cerebral cavernous malformations (CCM1) pathogenesis. *Hum. Mol. Genet.* 11:389–396.

Zawistowski, J.S., L. Stalheim, M.T. Uhlik, A.N. Abell, B.B. Ancrile, G.L. Johnson, and D.A. Marchuk. 2005. CCM1 and CCM2 protein interactions in cell signaling: implications for cerebral cavernous malformations pathogenesis. *Hum. Mol. Genet.* 14:2521–2531.

Zhang, J., R.E. Clatterbuck, D. Rigamonti, D.D. Chang, and H.C. Dietz. 2001. Interaction between krit1 and icap1alpha infers perturbation of integrin beta1-mediated angiogenesis in the pathogenesis of cerebral cavernous malformation. *Hum. Mol. Genet.* 10:2953–2960.

Zhang, J., D. Rigamonti, H.C. Dietz, and R.E. Clatterbuck. 2007. Interaction between krit1 and malcavernin: implications for the pathogenesis of cerebral cavernous malformations. *Neurosurgery*. 60:353–359.

Zhang, Z., H. Rehmann, L.S. Price, J. Riedl, and J.L. Bos. 2005. AF6 negatively regulates Rap1-induced cell adhesion. *J. Biol. Chem.* 280:33200–33205.